

Article

Detecting Fire-Caused Forest Loss in a Moroccan Protected Area

Iliana Castro ¹, Amanda B. Stan ¹, Lahcen Taiqui ² , Erik Schiefer ¹ , Abdelilah Ghallab ³, Mchich Derak ³ and Peter Z. Fulé ^{4,*} 

¹ Department of Geography, Planning and Recreation, Northern Arizona University, Flagstaff, AZ 86011, USA; imc49@nau.edu (I.C.); amanda.stan@nau.edu (A.B.S.); erik.schiefer@nau.edu (E.S.)

² Department of Biology, Faculty of Sciences of Tetouan, University Abdelmalek Essaâdi, Tétouan 93002, Morocco; Itaiqui@uae.ac.ma

³ Direction Régionale des Eaux et Forêts et de la Lutte Contre la Désertification du Rif à Tétouan, 33, Av. Mohamed V, Tétouan 93002, Morocco; a.ghallab@eauxetforets.gov.ma (A.G.); mchich78@gmail.com (M.D.)

⁴ School of Forestry, Northern Arizona University, Flagstaff, AZ 86011, USA

* Correspondence: pete.fule@nau.edu; Tel.: +1-928-523-1463

Abstract: Fire is a concern for the sustainability of dry forests such as those of the Mediterranean region, especially under warming climate and high human use. We used data derived from Landsat and MODIS sensors to assess forest changes in the Talassemtane National Park (TNP) in North Africa from 2003–2018. The Talassemtane National Park is a protected area in northern Morocco, a biodiverse, mountainous region with endemic species of concern such as the Moroccan fir (*Abies marocana*) and Barbary macaque (*Macaca sylvanus*). To help the managers of the TNP better understand how the forest has been impacted by fire vs. other disturbances, we combined information from remotely derived datasets. The Hansen Global Forest Change (GFC) data are a global resource providing annual forest change, but without specifying the causes of change. We compared the GFC data to MODIS wildfire data from Andela's Global Fire Atlas (GFA), a new global tool to identify fire locations and progression. We also analyzed surface reflectance-corrected Landsat imagery to calculate fire severity and vegetation death using Relative Differenced Normalized Burn Ratio analysis (RdNBR). In the park, GFC data showed a net loss of 1695 ha over 16 years, corresponding to an approximately 0.3% annual loss of forest. The GFA identified nine large fires that covered 4440 ha in the study period, coinciding with 833 ha of forest loss in the same period. Within these fires, detailed image analysis showed that GFA fire boundaries were approximately correct, providing the first quantitative test of GFA accuracy outside North America. High-severity fire, as determined by RdNBR analysis, made up about 32% of burned area. Overall, the GFA was validated as a useful management tool with only one non-detected wildfire in the study period; wildfires were linked to approximately 49% of the forest loss. This information helps managers develop conservation strategies based on reliable data about forest threats.

Keywords: Landsat; MODIS; Global Fire Atlas; Hansen Global Forest Change; forest loss; fire severity



Citation: Castro, I.; Stan, A.B.; Taiqui, L.; Schiefer, E.; Ghallab, A.; Derak, M.; Fulé, P.Z. Detecting Fire-Caused Forest Loss in a Moroccan Protected Area. *Fire* **2022**, *5*, 51. <https://doi.org/10.3390/fire5020051>

Academic Editors: Daniela Stroppiana, Mirco Boschetti and Alistair M. S. Smith

Received: 26 January 2022

Accepted: 7 April 2022

Published: 9 April 2022

Publisher's Note: MDPI stays neutral with regard to jurisdictional claims in published maps and institutional affiliations.



Copyright: © 2022 by the authors. Licensee MDPI, Basel, Switzerland. This article is an open access article distributed under the terms and conditions of the Creative Commons Attribution (CC BY) license (<https://creativecommons.org/licenses/by/4.0/>).

1. Introduction

Climate change poses challenges for forest sustainability by altering precipitation rates and average temperatures [1], which will affect forest types differently and have distinct management implications. Altered disturbances such as wildfire, insect and disease outbreaks, and drought are leading indicators of the changing climate's impacts on forests globally [2,3]. Some fire-dependent ecosystems such as those throughout much of western North America and Australia have experienced increasingly more frequent and severe fires in recent decades, although some Mediterranean Basin forests have seen variable patterns or even declines [4–8]. Rising temperatures in many areas are showing drought-induced reductions in the productivity of vegetation [9,10]. Interactions of disturbance and climate

change can increase the rate of tree mortality, damage to soil, and changes to overall forest structure [11]. Fire influences forest change in many interconnected ways including altered soils, carbon and hydrological cycles [12–14]. Forest loss is of critical concern because people all over the world rely on forest ecosystems for resources such as timber, wild harvest, spiritual and religious needs, and many other ecosystem services [15,16]. Human pressures such as grazing, logging, urban expansion, altered fire regimes, and agriculture have disturbed forest ecosystems, which have often degraded forests.

Remotely sensed data is a valuable resource for better understanding the dynamics of forests to develop improved strategies for reducing loss. Hansen et al. [17] created a dataset to map all forest change beginning in 2000 using Landsat time-series imagery at a spatial resolution of 30 m; the map currently has coverage through 2020. The Hansen Global Forest Change (GFC) data have been widely used to measure deforestation, contributing to national and global forest resource inventories and carbon accounting [18]. However, forest change can occur due to many different factors, including land clearing, wildfires, insect or disease outbreaks, or drought stress. Understanding the specific roles of different factors is valuable information that managers and governments can use to develop targeted science-based strategies for forest protection.

Wildfire activity can be directly monitored in real-time through MODIS (Moderate Resolution Imaging Spectroradiometer) satellite imagery. MODIS is an instrument on the Terra and Aqua satellites that gathers data on the entire Earth's surface every 1–2 days. The Global Fire Atlas (GFA) is one of several recently published databases that integrates MODIS data over time to map fires, creating ongoing measurements of the duration and progress of individual events and base information for calculating the contemporary fire regime [19–21]. The GFA provides data on fires globally from 2003–2018 (through July of 2018, our time of writing), created using MODIS burned-area data at a lower spatial resolution of 500 m [19].

Wildfire effects, such as spatial patterns of fire severity, can be derived from other sensors that detect reflectance changes due to vegetation mortality. Imagery from Landsat sensors is widely used to derive burn severity metrics such as the delta normalized burn ratio (dNBR) and its relativized form (RdNBR) [22]. Both the dNBR and RdNBR are based on the normalized burn ratio (NBR), which is an index derived by calculating the ratio between the near infrared (NIR) and shortwave infrared (SWIR) portions of the electromagnetic spectrum [23]. The RdNBR, developed by Miller and Thode [22], with a recent update by Parks et al. [24], has two advantages over an absolute index: (1) relative indices provide a more consistent definition of severity which allows better comparison of fires across space and time, and (2) classifying from a relative index should result in higher accuracy in heterogeneous landscapes.

The Mediterranean region is a culturally rich and diverse area that has been heavily shaped by human influences [25,26] and is characterized by a prominent role of fire [27]. Fires in North Africa are particularly prevalent close to the Mediterranean Sea, where the climate is sufficient in humid to subhumid regions for abundant fuel production [6]. Intensive land use by rural residents affects forest resources through land-clearing, grazing, and fire [5,28].

Forests in the Talassemtane National Park (TNP) in the Rif Mountains of Morocco in northwestern Africa, a critical habitat for several endangered species, are threatened by wildfires and land clearing for agricultural purposes. The area was set aside as a botanical reserve in 1972, designated a national park in 2004, and incorporated in the Mediterranean Intercontinental Biosphere Reserve by UNESCO in 2006 [29]. It is a mountainous area with small communities located in the valleys. The large changes in elevation allow many different vegetation types to be present within the boundary of the park, making this a highly biodiverse area [30]. Endangered or rare species in the park include the endemic Moroccan fir (*Abies marocana* Trab.), one of only two forests with *Abies* in Africa, as well as the black pine of the Atlas Mountains (*Pinus nigra* subsp. *mauretanica* Maire and Peyerimoff) and the Barbary macaque (*Macaca sylvanus*). Cannabis was grown traditionally

in limited quantities, but its cultivation was transformed by imported high-yield varieties and intensive agricultural production since the mid-2000s [31]. Forest clearing and fires associated with cannabis cultivation are considered the “main driver” of forest loss in the park [30].

We used multiple sources of remotely sensed data to quantify the role of wildfires as a factor of forest loss over a 16-year period, 2003–2018 in TNP. We combined the Global Forest Change data, the Global Fire Atlas data, vegetation coverages provided by the Moroccan Department of Water and Forests, and processed Landsat satellite data, to determine the role of fire in overall forest change from 2003–2018. Our goal was not to detect every ignition on the landscape, but rather to identify relatively large/severe fires that were associated with detectable forest loss. A key challenge is that different data sets may have distinct resolutions, precisions, and definitions of “forest”, adding complications to comparisons. However, such issues are ubiquitous in the application of remotely sensed data. In our study, combining data sets can help forest managers better understand the current forest impacts in the park and highlight areas that are of high concern.

Our objectives were:

1. Compare and analyze overall forest loss (GFC) and large wildfires (GFA) annually from 2003–2018.
2. Assess the GFA fires with before/after-fire Landsat imagery and examine fire severity using RdNBR.
3. Determine the overall contribution of wildfire to forest loss at TNP, particularly in the rare *Abies* forest, providing actionable information to park managers.

2. Materials and Methods

2.1. Study Area

The study area is Talassemtane National Park (TNP) in northwestern Morocco near the city of Chefchaouen and the Mediterranean Sea (Figure 1). The area of the park is approximately 58,000 ha, with about 75% occupied by forest lands [32]. The climate in TNP is Mediterranean, characterized by cool and rainy winters while summers are hot and dry. The average rainfall is 942 mm per year and the average temperature is 16. °C at the weather station in Chefchaouen, which is at an elevation of 630 m [33]. Average rainfall is 1248 mm per year and the average temperature is 14.9 °C at the Bab Taza weather station at 880 m elevation [32]. Average rainfall is estimated at 1705 mm per year and average temperature is estimated at 11.0 °C at the high-elevation zone between 1400–2000 m of fir forest or *Sapinière*, dominated by *Abies* [32]. There are an estimated 1380 plant species in the park, 314 of which are endemic to Morocco, and 86 are endemic to the park [34]. The dominant forest types (Figure 1) are Moroccan fir and black pine (*Abies marocana* and *Pinus nigra*), *Cedrus atlantica* (Endl.) Carrière, and maritime pine (*P. pinaster* Aiton) forest intermixed with many different oak species (e.g., *Quercus rotundifolia* Lam., *Q. faginea* Lam., and *Q. suber* L.), while the lower elevation of the park is composed mostly of *Tetraclinis articulata* (Vahl) Mast. and matorral shrubs [34]. The forest types mapped by the Moroccan Department of Water and Forests are based on aerial photo interpretation and field reconnaissance circa 2004 (Figure 1). The map includes areas of “forest” stands as well as “forest + matorral” shrub areas where isolated trees or clumps dominate a contiguous shrub midstory. The subjective nature of the difference between “forest” vs. “forest + matorral shrub” made it impossible to separate the mapped forests by canopy cover for direct comparison with the GFC data [17] described below.

The lower slopes of the mountains have been heavily cultivated for agricultural purposes, especially for high yields of cannabis production since the mid-2000s [31]. Agriculture is encroaching into higher reaches of the mountains, deforesting pine and threatening fir forests. The use of fire is a historical practice for clearing land for agricultural purposes [35] but can be used improperly and start forest fires.

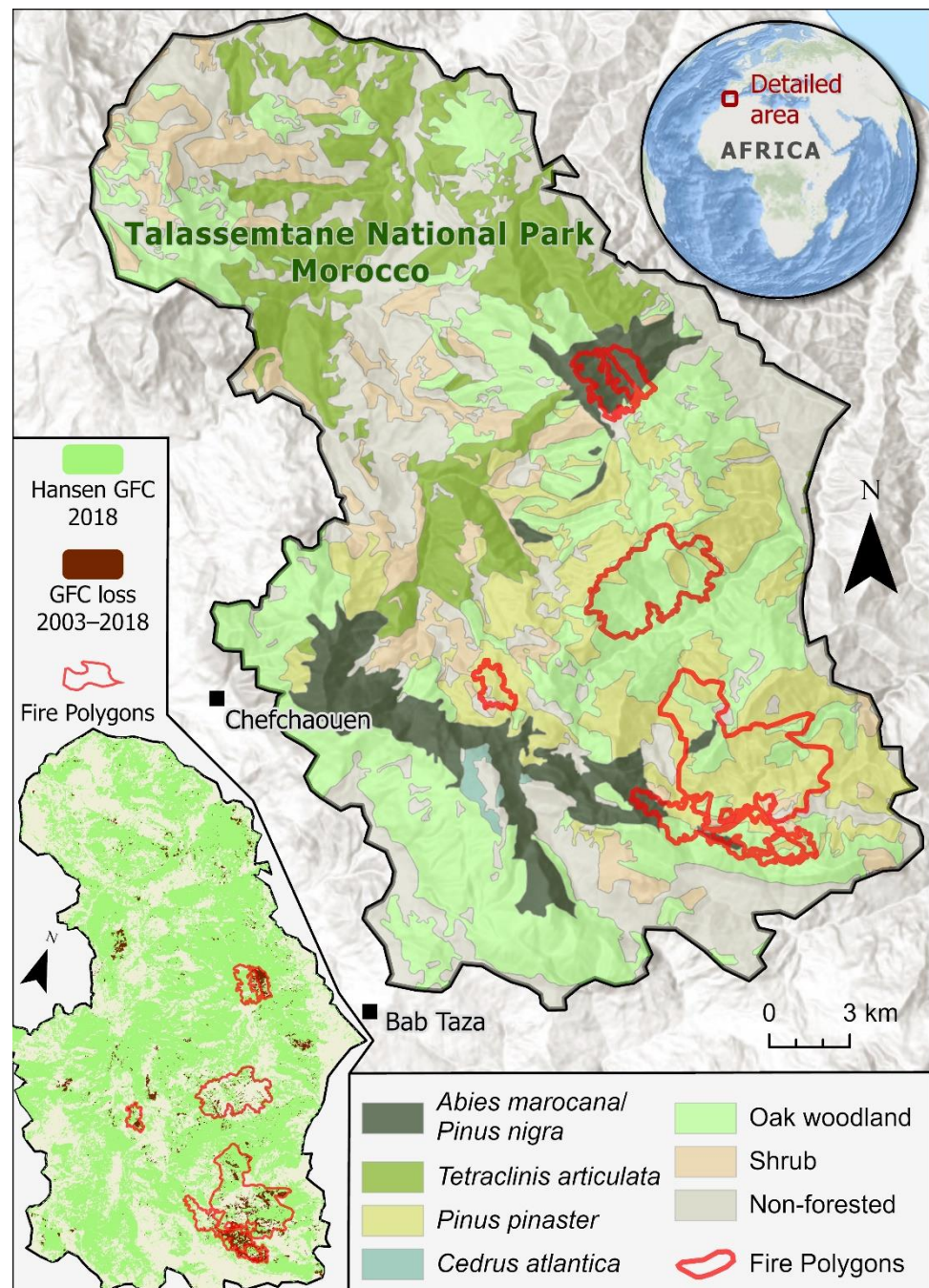


Figure 1. Talassemtane National Park with forested vegetation and fire polygons. Inset: Global Forest Change (GFC) map showing forested area, forest loss over the study period (2003–2018), and fire polygons.

2.2. Global Forest Change (GFC) Data

Disturbance-induced change in forest composition occurs often, whether it be a stand-replacing forest fire or a timber harvest. Forest disturbances are picked up indiscriminately by the GFC algorithm [17] to estimate global-scale forest change. This data product maps forest cover extent and loss between 2000 through the present using Landsat data at a spatial resolution of 30 m. The forest changes in the GFC dataset are not attributed to any specific causes. Loss is defined as a stand-replacing disturbance or complete removal of tree canopy cover more than 5 m in height with a minimum 25% coverage at the Landsat pixel level, with no distinction between forest types or species. Loss is updated annually.

In the present study, we used the GFC data set to estimate total forest losses (ha) by year from 2003 to 2018 in Talassemthane National Park. Annual losses were derived based on the mapped extent of forest cover in 2003 in TNP and do not include forest gains during the period of study. We compared the GFC data to the Global Fire Atlas (GFA) data to quantify the role of fire as an agent of forest loss in the park.

2.3. Global Fire Atlas (GFA) Data

The Global Fire Atlas provides data on fires worldwide from 2003–2018 and was created using an analysis of the Collection 6 MCD64A1 MODIS burned area data product [36]. The near daily availability of MODIS data allows for quick updates on fires and detection of daily ignitions. The algorithm used in the GFA tracks daily progress of individual fires at 500 m resolution to create fire behavior metrics in raster and vector formats [19]. In the original publication, Andela et al. [19] reported that the algorithm detected 13.3 million individual fires globally over the study period, and they showed that specific individual test case fires had good agreement with other sources of fire information in the United States. While the GFA is potentially a useful tool worldwide, to our knowledge the present study is the first test case from outside North America. The data can be accessed freely at <https://www.globalfiredata.org/fireatlas.html> (accessed on 8 April 2022). Data can be downloaded by year for the entire globe. The attributes of the data include ignition date and location, size of the fire, perimeter, speed, direction of spread, and duration. However, fire severities are not defined in the data. The 500 m resolution of GFA is coarser than the 30 m GFC data, but MODIS fire products are used by regional managers and many scientists due to the high data quality/consistency and the near real-time availability of such data on fire activity.

Fire boundaries for the GFA fires that occurred in the park from 2003–2016 were obtained using the data explorer tool on the GFA website. For every year that had a confirmed fire in or overlapping the park boundary, we downloaded the data in GIS-ready file formats (shapefiles) that show individual fire perimeters and ignition locations. Shapefiles for fires that occurred in 2017 and 2018 were obtained directly from N. Andela (pers. comm).

To assess potential omissions in the GFA [37], we used the Near real-time (NRT) Suomi National Polar-orbiting Partnership Visible Infrared Imaging Radiometer Suite (S-NPP/VIIRS) Active Fire detection product (VNP14IMGTDL_NRT) at a 375 m resolution (<https://earthdata.nasa.gov/earth-observation-data/near-real-time/firms/v1-vnp14imgt>, accessed on 6 April 2022) [38]). Fires from this product were coupled with the GFA fires that occurred in the park from 2012–2018, the period of overlap between the two data sets. Secondly, this product allowed us to examine the frequency and spatial distribution of small fires in the park to understand how they impact forest loss compared to larger fires, the latter of which have a much greater ecological impact and are the primary focus of this study. Analyses of fires from the VIIRS NRT active fire data product are provided in the Supplementary Material.

2.4. NBR and RdNBR

We calculated fire severity and vegetation change using the Normalized Burn Ratio (NBR) and Relativized delta Normalized Burn Ratio (RdNBR) using Landsat 5 Thematic Mapper (TM), Landsat 7 ETM+ and Landsat 8 Operational Land Imager (OLI) Tier 2 surface reflectance products. Fire analysis using before/after-fire Landsat pairs is recognized as a valid technique for assessing MODIS-detected burned areas [39]. Surface reflectance data have been adjusted for atmospheric effects using atmospheric correction algorithms to have a Bottom of Atmosphere view (BOA), which can improve results in change detection [40]. We used multiple satellites due to the changes in satellite availability over the study period. We picked Landsat scenes using the dates provided by the Global Fire Atlas for each individual fire within the park. A scene was selected pre- and post-fire with the lowest cloud cover available. Post-fire images were within one year of the end date of the fire.

Scenes were picked during the summer months (end of June-mid September) to minimize effects from seasonal change in foliage. The area of the park falls within one Landsat scene (Path 201, Row 036), so only one scene was needed for pre- and post-fire for every fire detected (Table 1, Figure 2).

Table 1. Dates of fires detected by the Global Fire Atlas (GFA) and Landsat (LS) imagery used to assess fire severity.

GFA Fire Years	GFA Start Date	GFA End Date	Landsat Satellite	Pre-Fire LS Date	Post-Fire LS Date
2003	14 August 2003	17 August 2003	5	22 July 2003	8 July 2004
	18 August 2003	30 August 2003	5	22 July 2003	8 July 2004
2007	19 November 2007	30 November 2007	5	17 July 2007	20 August 2008
	20 November 2007	29 November 2007	5	17 July 2007	20 August 2008
2012	14 September 2012	2 October 2012	7	7 August 2012	11 September 2013
2014	17 September 2014	22 September 2014	8	6 September 2014	21 June 2015
2015	14 July 2015	17 July 2015	8	21 June 2015	23 July 2015
2017	19 September 2017	19 September 2017	8	14 September 2017	29 June 2018
2018	2 August 2018	3 August 2018	8	29 June 2018	18 July 2019

We calculated NBR using the near infrared (NIR) and shortwave infrared (SWIR) wavelengths. The bands for NIR are different for Landsat 5, 7, and 8 as follows:

For Landsat 5–7 TM and ETM+, $NBR = (Band\ 4 - Band\ 7) / (Band\ 4 + Band\ 7)$.

For Landsat 8 OLI, $NBR = (Band\ 5 - Band\ 7) / (Band\ 5 + Band\ 7)$.

We calculated dNBR as the difference between the NBR from pre-fire and post-fire images. dNBR values were multiplied by 1000 and converted to integer format. We calculated RdNBR using the formula of Miller and Thode [22]:

$$RdNBR = dNBR / |(NBR_{prefire})|^{0.5}$$

We digitized fire polygons using the RdNBR rasters displayed at a 4:1 resolution (monitor pixel:raster cell). Digitizing was achieved following contiguous burned pixels that showed sharp contrast to adjacent pixels. Areas that had sharp contrast within the larger polygons were included as part of the polygon and not eliminated. For the one fire in 2012 that was mapped using Landsat 7 ETM+ imagery, we interpolated the polygon boundary across the gaps created by the Scan Line Corrector (SCL-off) anomaly.

We clipped our digitized fire polygons to the previous year's forest coverage according to the GFC dataset. This allowed us to estimate the amount of forest within our polygons each year. We then estimated the area considered "loss" by GFC within our fire polygons. As the GFC dataset represents median, cloud-free pixel values over a growing season, forest loss within a given calendar year might be recorded in the year the loss occurred or in the year after. Therefore, we estimated loss within our polygons by calculating the difference between forest area in the year before the fire and the year after the fire.

We estimated the amount of high-severity fire in forested areas within our polygons. Because the GFC defines forest loss as occurring when tree cover declines below 25%, high-severity fire was likely to be most closely associated with forest loss [41]. Fire severity is defined by Key and Benson [23] as, "the quality or state of distress inflicted by a force. The magnitude of environmental change caused by a fire, or the resulting cost in socioeconomic terms". Severity is often difficult to quantify. For the present study, we focused on the environmental impacts of the fire which included physical and chemical changes to the soil, loss of vegetation, and changes to forest structure or composition. The USGS Landscape Assessment (LA) Sampling and Analysis Methods [23] recommends the use of ground measurements called the Composite Burn Index (CBI) to assess burn severity to validate the satellite data. However, CBI is not widely used in Africa, and no field CBI values exist for the fires that took place within the boundary of the TNP. The lack of ground data is a common situation affecting most satellite-based fire severity assessments, even in nations with more resources available [42]. Following standard practice, we used the modeled

RdNBR threshold for high severity (≥ 641) developed by Miller and Thode [22]. Their thresholds were developed based on CBI field data in Mediterranean-climate coniferous forests with shrub understories, relatively similar to those of our Moroccan study site. We also estimated the amount of high-severity fire in *Abies marocana*/*Pinus nigra* forest within our polygons using the vegetation coverage provided by the Moroccan Department of Water and Forests.

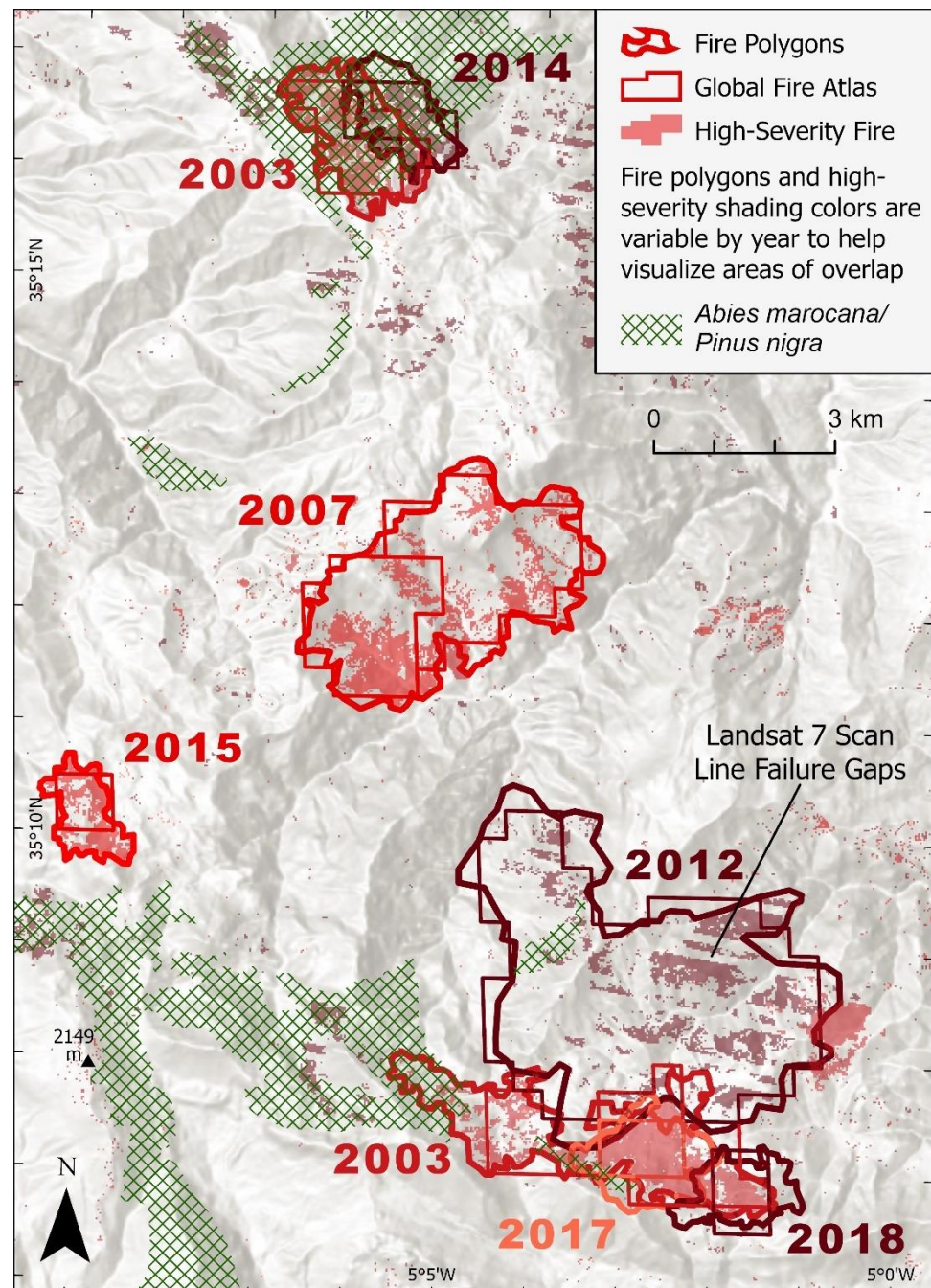


Figure 2. Comparison of Global Fire Atlas (GFA) polygons with fire perimeters digitized from Landsat-derived RdNBR rasters. Additionally, shown are high-severity burn patches and the distribution of *Abies*/*Pinus* forest.

3. Results

The first objective was to determine overall forest loss and area of large wildfires. Baseline forest conditions were not consistent between the GFC forest cover data for the TNP and the vegetation type coverage for the park, likely due to differences in the definitions of “forest.” The forest coverage from the Moroccan Department of Water and Forests (Figure 1) showed 43,633 ha of forest cover while GFC data showed 38,570 ha in 2003, a difference of 5063 ha between the base years of both datasets. The Moroccan map included areas of “forest + matorral shrub” which may have fallen below the minimum canopy cover requirement for the GFC map (25% canopy cover), possibly explaining the lower GFC forest area value. From 2003 to 2018, GFC data showed 1695 ha of forest loss in the TNP, approximately 4% loss of forest cover as defined by the 2003 GFC forest cover base year, over 16 years (Table 2). The average annual loss of forests according to the GFC data was 106 ha per year.

Table 2. Comparison from 2003–2018 of Global Forest Change (GFC), fires detected by the Global Fire Atlas (GFA), and fire areas assessed with Landsat (LS) imagery. Fire severity was assessed from LS images as described in the text.

Year	GFC Forest Loss (ha) *	GFA Fires; Area (ha); No. of Fires	LS Fires (ha)	LS Fires, Forested (ha) +	GFC Loss within LS Fires (ha)	LS Fires, Forested, High Severity (ha)	<i>Abies/Pinus</i> Forest Loss to High Severity Fire (ha)
2003	36	901; <u>2</u>	987	710	78	502	204
2004	104	<u>0</u>					
2005	23	<u>0</u>					
2006	6	<u>0</u>					
2007	156	1051; <u>2</u>	1115	432	91	337	0
2008	188	<u>0</u>					
2009	13	<u>0</u>					
2010	29	<u>0</u>					
2011	82	<u>0</u>					
2012	300	1951; <u>1</u>	2000	1407	329	518 **	7 **
2013	139	<u>0</u>					
2014	153	193; <u>1</u>	211	186	106	100	90
2015	46	86; <u>1</u>	145	109	31	78	0
2016	67	<u>0</u>					
2017	84	129; <u>1</u>	263	193	94	6	1
2018	269	129; <u>1</u>	175	142	104	4	0
Total	1695	4440; <u>9</u>	4896	3179	833	1545	302

* Starting forest cover from GFC for TNP in 2003 was 38,570 ha. + Amount of forest contained within our digitized polygons, based on GFC, and therefore subject to loss by fire in a given year. ** Area adjusted for the proportion of the fire polygon covered by the evenly-spaced Landsat 7 ETM+ line failure data gaps (28%). We used the percentage of high-severity fire in the area outside of the data gaps to estimate the percentage of high-severity fire within the gaps.

The GFA recorded nine wildfires in seven years over the 16-year period, with a total area of 4440 ha (Table 2). For years that fire was recorded in the GFA, total fire areas ranged from 86 to 1951 ha, with an average of 634 ha. In every year except 2018, the overall area of GFA polygons was greater than the total GFC loss in that year, even when the area of GFC loss in the year following the fire was included (before 2014). Possible explanations for the higher amount of GFA total area as compared to GFC total loss are the fact the GFA data are relatively coarser than GFC (500-m vs. 30-m pixels) and that fires have variable severity including non-lethal severities. Using the VIIRS NRT active fire data product for the period of overlap between the two datasets, 2012–2018, approximately 70 distinct fires (isolated points and synchronous clusters) were detected in the park. There were five GFA fires detected during that same period (Figure S1).

The second objective was to pair the GFA with Landsat imagery and examine fire severity using RdNBR. All nine fires identified by GFA were confirmed in Landsat scenes and fire areas were highly correlated. In all instances of comparing the fires, the GFA fire polygons extracted from 500 m resolution MODIS imagery had a lower area than the fire polygons we manually digitized from 30 m resolution Landsat imagery (4440 ha GFA, 4896 ha Landsat). However, the areas of GFA polygons were highly correlated with the areas of Landsat fire polygons ($r = 0.99$). The year with the lowest difference was 2012 (49 ha, 3%) and the greatest difference was in 2017 (134 ha, 51%) (Table 3). The average difference between the GFA and Landsat polygons was 65 ha with a total difference of 456 ha (9%) between the totals of the GFA and Landsat areas. Only one fire larger than a MODIS pixel was detected by a cluster of synchronous ignitions in the VIIRS NRT data but not by GFA (Figure S1). Analysis of this 2012 fire showed that it was associated with 53 ha of forest loss in GFC (Table S1).

Table 3. Differences in area (ha) and percent between the Landsat (LS) and GFA fire polygons, as well as between GFC forest loss and LS-high severity. Negative values mean the first variable was larger than the second.

Year	LS-GFA Difference, ha	LS-GFA Difference, %	LS-High Severity-GFC Loss, ha	LS-High Severity-GFC Loss, %
2003	86	8.7%	466	92.8%
2007	64	5.7%	181	53.7%
2012	49	2.5%	218	42.1%
2014	18	8.5%	−53	−53.0%
2015	59	40.7%	32	41.0%
2017	134	51.0%	−78	−1300%
2018	46	26.3%	−265	−6625%

Landsat fires included a total of 3179 ha of forested areas (Table 2). High-severity fire, as determined by RdNBR analysis, comprised 1545 ha or approximately 49% of the Landsat forested fire area. GFA fire areas were well-correlated with Landsat high-severity fire areas ($r = 0.90$), but the total of GFA fire polygons (4440 ha) was nearly three times larger than the total of high-severity fire (1545 ha).

The third objective, estimating the overall contribution of wildfire to forest loss at TNP, is based on multiple perspectives due to the different data sets involved. Overall, GFA and Landsat fires were highly similar in total area burned over the 16-year period, approximately 4700 ha. However, GFA fires included non-forested areas. Restricting the analysis to forested areas, Landsat fires covered 3179 ha or about 7% of the initial forested area (43,633 ha) based on the Moroccan forest management map, corresponding to an average of 199 ha/year. Converting the fire occurrence into an overall fire regime statistic, the fire rotation (time required to burn an area equivalent to the entire forested area) would be 219 years. Using the smaller GFC forest map (38,570 ha), the fire rotation would be 193 years. The preceding calculations are generalizations that do not take into account relief, differences in forest composition, soil, or land use, so they should be considered as rough approximations.

However, these burned areas did not uniformly result in forest loss. Of the overall GFC loss in the park (1695 ha), 833 ha (49%) were within the Landsat fire polygons, corresponding to a 1.9–2.2% loss of total forest cover compared to 2003 values for the Moroccan forest map or the GFC forest map. Taking 2% as an average value, the annual average fire-associated loss over the 16-year period would be 0.13%/year. This value is likely a minimum because high-severity fire from Landsat analysis was about twice as high (1545 ha vs. 833 ha).

The rarest endemic forest type in the region, *Abies maroccana*/*Pinus nigra*, was disproportionately affected by fire. The area of *Abies/Pinus* forest was 4766 ha at the start of the

study period in 2003, including *Abies* + matorral shrub. Of this area, 302 ha (6.3%) were lost within the perimeters of high-severity fire during the study period (Table 2).

4. Discussion

4.1. Forest Loss and Fire

The overall annual average forest loss in the park from 2003–2018 averaged 106 ha/year, ranging from 6 to 300 ha/year, using GFC data. While relatively small at an average of about 0.3% forest loss per year, evidence of instability is of concern because the forests of the TNP are unique in North Africa and provide critical habitat for many species, protection of water resources, ecotourism to stimulate the local economy, and traditional medicine to local people [43,44]. Despite being a protected area, the TNP trend in forest loss is consistent with the average trend of deforestation estimated in the surrounding region during the second half of the 20th century, about 0.3% per year [45].

Fire played a notable role in the forested ecosystems of Talessemtane National Park in the early twenty-first century, with GFA data showing an average of 278 ha burned per year between 2003–2018. Knowing where forest loss is happening, and better understanding the role of severe wildfires, is valuable information when deciding how to manage a protected area. Identifying areas with high impact can bring attention to areas in need of post-fire rehabilitation.

Comparison of the MODIS-based GFA data with detailed before-after Landsat analysis using RdNBR suggests that the GFA and similar MODIS products offer a fast and straightforward technique for fire estimation. The GFA closely matched Landsat fire areas; estimates of area differed by about 20% with GFA consistently lower, but the two methods were highly correlated ($r = 0.99$), although with a low number of years, $n = 7$. High consistency was also reported in a previous test of GFA fires with burned area analysis using Landsat data in the Monitoring Trends in Burn Severity (MTBS) program in the USA [19]. Recently Balch et al. published a new algorithm for interpreting MODIS fire data in fire atlas form in the USA [20] and other studies are emerging on MODIS accuracy [46,47]. To our knowledge, the present study is the first comparison of the GFA specifically with Landsat RdNBR and forest loss data outside of North America, but researchers are increasingly comparing and cross-validating fire and forest datasets [21,48–50].

The two techniques provide similar data about burned area, but GFA has several advantages, including automated data collection and specific dates of fire initiation and termination. The MODIS sensor records fire at a near-daily time scale. Using the data explorer tool on the GFA website, managers can rapidly estimate fire frequency, peak fire season, and estimate fire regime statistics such as fire rotation. However, as GFA data are limited to estimates of fire progression and overall perimeters, fire severity estimates require Landsat or similar data for calculation of RdNBR or other severity metrics [22].

Integrating forest loss and fire data showed that fire was clearly associated with forest loss, with approximately half of the GFC forest loss during the study period occurring within the perimeters of fires. The fire-associated loss at TNP is somewhat higher than global values, as an average of $38 \pm 9\%$ of forest loss worldwide was associated with fire in the same time period [51]. Fire at TNP was linked with an average of approximately 0.13% of forest loss/year. Differences in the data resolution and in definitions applied in the creation of forest maps make comparisons imperfect, but the different estimates are consistent in magnitude. Overall fire rotation calculations resulted in a range of 193–219 years required to burn an area equivalent to the total forested area. However, the different forest types vary widely in fire adaptations, fuel types, fuel moisture, and other attributes, so more detailed studies of specific fire regimes within forest types would be useful for better understanding of the ecological role of fire, especially in the case of low-severity fires that are not detected well by satellite-borne sensors.

Fire was a particular threat to the rarest forest type, the endemic *Abies marocana*/*Pinus nigra*, with over 6% loss within high-severity fires during the study period. While *Abies* forests in general are often characterized by infrequent but severe stand-replacing fire regimes

with adaptations for post-fire regeneration [52], special attention is warranted in the case of a highly restricted, rare species such as *A. marocana* [53]. Mapping of the severe fire area could be applied to post-fire surveys of regeneration, for example, to assess the recovery trajectory of the burned area.

By distinguishing which areas were not affected by fire, the non-burned GFC data can be used by managers to indicate areas that are potentially being targeted for agricultural expansion. Areas outside of the fire polygons that show loss could identify areas being encroached upon by agriculture. Paired with the vegetation coverages, the GFC and GFA data can highlight areas where important forest types are being lost to help conserve biodiversity in the park. For example, a study using similar techniques in Brazil recently reported increased deforestation and fire in the Chico Mendes Reserve, arguing for increased global attention to the threats to biodiversity [54].

4.2. Limitations

Attempts to reconstruct fires and forest change on large landscapes over time are inherently challenging, especially where resources for field assessments are limited. However, this situation is common across most of the world. It is fortunate that remotely sensed data on fire and forests are widely and freely available, especially when organized through user-friendly packages such as GFC and GFA.

Key limitations of this study were the differences in spatial data resolution and in development of forest maps, as discussed in Section 2. We dealt with these limitations by bracketing results by minimum and maximum measures of forest area. Results regarding forest loss associated with fire differed in magnitude but were relatively consistent across different forest definitions (GFC forest map vs. Moroccan forest management map), lending confidence to interpretations for management.

The means of fire detection used in this study, MODIS for detection of energy released by combustion, and Landsat for before–after comparisons of vegetation change, are most accurate at identifying relatively severe burns. A global validation study found that MODIS-detected burned area tended to be smaller than Landsat-derived burned area [39], which matches our findings at TNP. Importantly, both methods are less likely to detect fires that primarily burn as low-intensity surface fires [39]. Low-severity fires may not emit enough energy to be picked up by the MODIS sensor or affect forest structure severely enough to trigger forest loss through the GFC algorithm, but surface fires can play important ecological roles [55]. Field measurement of fire-affected sites across a range of fire severities, coupled with tree-ring-based studies of fire occurrence and severity that can provide data much farther back in time, would be valuable information for developing conservation strategies across scales from individual trees to landscapes.

One region in the southeastern area of the park had four fires that overlapped during the study period. Overlapping fires may have resulted in inaccuracies in total forest cover/forest loss from the GFC data. In 2017 and 2018, the high severity area was much lower than the forest loss area, possibly linked to the overlap in the fire areas. During the overlapping period when VIIRS NRT data and GFA data were both available (2012–2018), only one fire larger than a MODIS pixel was not detected in the GFA dataset. The VIIRS NRT product picks up more individual ignitions than the coarser-scale MODIS product. Fires that are small in area and/or of low intensity may have important ecological effects, especially in relatively dry forests characterized by frequent, low severity fire regimes, adding to the utility of our recommendation for additional field study of fire ecology. However, in the context of the present study on forest loss, only 53 ha of GFC forest loss was associated with the fire not detected in the GFA, representing 5% of the total forest loss during the period of overlap between the GFA and VIIRS NRT data sets (2012–2018).

4.3. Conclusions

Baseline data on how and why forest loss occurs can help managers understand current trends brought on by human activities and warming climate. Using multiple

remote sensing data sets, we were able to compare the forest loss and fires over 16 years in the TNP, identifying severe wildfires as the likely proximal cause for about half of the forest loss. The park has undergone forest loss averaging 106 ha/year, approximately 0.3% of forest area, annually. While still a relatively small value, the high value of unique, fire-vulnerable forest ecosystems in the TNP merits management attention. Additional research on fire ecology of individual ecosystem types over the rugged topographic gradient of the park, coupled with analysis of climate-fire-forest relationships, would be beneficial to reduce threats of increasing forest loss. The fact that approximately half the forest loss is *not* associated with fire indicates that it would be beneficial to managers and social scientists to address tree cutting, agricultural expansion, and the socioeconomic factors driving human activities in the TNP and surrounding landscape. The combination of free and user-friendly datasets applied in this study is beneficial across many landscapes worldwide to understand the role of fire in forest loss.

Supplementary Materials: The following are available online at <https://www.mdpi.com/article/10.3390/fire5020051/s1>, Figure S1: Analysis of forest loss and fires from the Near real-time (NRT) Suomi National Polar-orbiting Partnership Visible Infrared Imaging Radiometer Suite (S-NPP/VIIRS) Active Fire detection product (VNP14IMGTDL_NRT) at a 375 m resolution. The improved spatial resolution and high fidelity of the VIIRS NRT active fire data product (<https://earthdata.nasa.gov/earth-observation-data/near-real-time/firms/v1-vnp14imgt>, accessed on 6 April 2022) results in a significantly greater quantity of detected fires relative to MODIS-based fire products. Approximately 70 distinct fires (isolated points and synchronous clusters) were detected in the park for the period 2012–2018. Most isolated fire detection points correspond with zero to a few pixels (Landsat resolution, 30 m) of recorded Hansen forest loss over the same analysis period. A few synchronous point clusters correspond with larger fragments of Hansen forest loss, but still at a scale much finer than our MODIS pixel analysis level. One large cluster of VIIRS active fire points corresponds with a 2012 (August) fire with an extent exceeding one MODIS pixel. That fire was mapped and assessed for burn severity and other fire parameters consistent with GFA fires (Table 2). * Extents of clustered, synchronous VIIRS fire points outside GFA fires were visually assessed by cross-referencing Landsat imagery before and after burning; Table S1: Fire parameters (c.f. Table 2) of the 12 August 2012 VIIRS detected, non-GFA dataset fire identified in Figure S1. Landsat imagery used to assess fire severity (RdNBR): 7 August 2012 (pre-fire; Landsat 7); 18 August 2013 (post-fire; Landsat 8).

Author Contributions: Conceptualization, P.Z.F., L.T., M.D. and A.B.S.; methodology, I.C., A.B.S., P.Z.F., E.S. and A.G.; formal analysis, I.C., A.B.S. and P.Z.F.; data curation, I.C. and A.B.S.; writing—original draft preparation, I.C., A.B.S. and P.Z.F.; writing—review and editing, all authors; supervision, P.Z.F. and A.B.S.; project administration, A.B.S. and P.Z.F.; and funding acquisition, A.B.S., E.S. and P.Z.F. All authors have read and agreed to the published version of the manuscript.

Funding: This research was funded in part by a Fulbright Scholar grant to P.Z.F. through the Moroccan-American Commission for Educational & Cultural Exchange (MACECE) and funding from the Charles O. and Mary Minor Professorship, School of Forestry, Northern Arizona University, as well as scholarships to I.C. from the Department of Geography, Planning and Recreation, Northern Arizona University.

Institutional Review Board Statement: Not applicable.

Informed Consent Statement: Not applicable.

Data Availability Statement: Imagery is publicly available as described in the text. Landsat imagery from the USGS EarthExplorer (<https://earthexplorer.usgs.gov/>, accessed 6 April 2022) website. Data from analyses carried out in the study are archived at Northern Arizona University and are available from the authors upon request.

Acknowledgments: We thank Talassemtane National Park, Abdelmalek Essaâdi University, and the Département des Eaux et Forêts—Maroc.

Conflicts of Interest: The authors declare no conflict of interest. The funders had no role in the design of the study; in the collection, analyses, or interpretation of data; in the writing of the manuscript, or in the decision to publish the results.

References

1. Valdes-Abellan, J.; Pardo, M.A.; Tenza-Abril, A.J. Observed Precipitation Trend Changes in the Western Mediterranean Region. *Int. J. Climatol.* **2017**, *37*, 1285–1296. [[CrossRef](#)]
2. Nagel, L.M.; Palik, B.J.; Battaglia, M.A.; D'Amato, A.W.; Guldin, J.M.; Swanston, C.W.; Janowiak, M.K.; Powers, M.P.; Joyce, L.A.; Millar, C.I.; et al. Adaptive Silviculture for Climate Change: A National Experiment in Manager-Scientist Partnerships to Apply an Adaptation Framework. *J. For.* **2017**, *115*, 167–178. [[CrossRef](#)]
3. Seidl, R.; Thom, D.; Kautz, M.; Martin-Benito, D.; Peltoniemi, M.; Vacchiano, G.; Wild, J.; Ascoli, D.; Petr, M.; Honkaniemi, J.; et al. Forest Disturbances under Climate Change. *Nat. Clim. Chang.* **2017**, *7*, 395–402. [[CrossRef](#)] [[PubMed](#)]
4. Liu, Y.; Stanturf, J.; Goodrick, S. Trends in Global Wildfire Potential in a Changing Climate. *For. Ecol. Manag.* **2010**, *259*, 685–697. [[CrossRef](#)]
5. Chergui, B.; Fahd, S.; Santos, X.; Pausas, J.G. Socioeconomic Factors Drive Fire-Regime Variability in the Mediterranean Basin. *Ecosystems* **2018**, *21*, 619–628. [[CrossRef](#)]
6. Curt, T.; Aini, A.; Dupire, S. Fire Activity in Mediterranean Forests (The Algerian Case). *Fire* **2020**, *3*, 58. [[CrossRef](#)]
7. European Commission; Joint Research Centre. *Forest Fires in Europe, Middle East and North Africa 2018*; Publications Office: Luxembourg, 2019.
8. Belhadj-Khedher, C.; Koutsias, N.; Karamitsou, A.; El-Melki, T.; Ouelhazi, B.; Hamdi, A.; Nouri, H.; Mouillot, F. A Revised Historical Fire Regime Analysis in Tunisia (1985–2010) from a Critical Analysis of the National Fire Database and Remote Sensing. *Forests* **2018**, *9*, 59. [[CrossRef](#)]
9. Thripleton, T.; Bugmann, H.; Folini, M.; Snell, R.S. Overstorey–Understorey Interactions Intensify After Drought-Induced Forest Die-Off: Long-Term Effects for Forest Structure and Composition. *Ecosystems* **2018**, *21*, 723–739. [[CrossRef](#)]
10. O'Connor, C.D.; Falk, D.A.; Lynch, A.M.; Swetnam, T.W.; Wilcox, C.P. Disturbance and Productivity Interactions Mediate Stability of Forest Composition and Structure. *Ecol. Appl.* **2017**, *27*, 900–915. [[CrossRef](#)]
11. O'Connor, C.D.; Falk, D.A.; Garfin, G.M. Projected Climate-Fire Interactions Drive Forest to Shrubland Transition on an Arizona Sky Island. *Front. Environ. Sci.* **2020**, *8*, 137. [[CrossRef](#)]
12. Jones, M.W.; Santín, C.; van der Werf, G.R.; Doerr, S.H. Global Fire Emissions Buffered by the Production of Pyrogenic Carbon. *Nat. Geosci.* **2019**, *12*, 742–747. [[CrossRef](#)]
13. Pingree, M.R.A.; DeLuca, T.H. The Influence of Fire History on Soil Nutrients and Vegetation Cover in Mixed-Severity Fire Regime Forests of the Eastern Olympic Peninsula, Washington, USA. *For. Ecol. Manag.* **2018**, *422*, 95–107. [[CrossRef](#)]
14. Rust, A.J.; Saxe, S.; McCray, J.; Rhoades, C.C.; Hogue, T.S. Evaluating the Factors Responsible for Post-Fire Water Quality Response in Forests of the Western USA. *Int. J. Wildland Fire* **2019**, *28*, 769. [[CrossRef](#)]
15. Sodhi, N.S.; Lee, T.M.; Sekercioglu, C.H.; Webb, E.L.; Prawiradilaga, D.M.; Lohman, D.J.; Pierce, N.E.; Diesmos, A.C.; Rao, M.; Ehrlich, P.R. Local People Value Environmental Services Provided by Forested Parks. *Biodivers. Conserv.* **2010**, *19*, 1175–1188. [[CrossRef](#)]
16. Córdova, J.P.P.; Wunder, S.; Smith-Hall, C.; Börner, J. Rural Income and Forest Reliance in Highland Guatemala. *Environ. Manag.* **2013**, *51*, 1034–1043. [[CrossRef](#)]
17. Hansen, M.C.; Potapov, P.V.; Moore, R.; Hancher, M.; Turubanova, S.A.; Tyukavina, A.; Thau, D.; Stehman, S.V.; Goetz, S.J.; Loveland, T.R.; et al. High-Resolution Global Maps of 21st-Century Forest Cover Change. *Science* **2013**, *342*, 850–853. [[CrossRef](#)]
18. Allen, C.D.; Breshears, D.D.; McDowell, N.G. On Underestimation of Global Vulnerability to Tree Mortality and Forest Die-off from Hotter Drought in the Anthropocene. *Ecosphere* **2015**, *6*, art129. [[CrossRef](#)]
19. Andela, N.; Morton, D.C.; Giglio, L.; Paugam, R.; Chen, Y.; Hantson, S.; van der Werf, G.R.; Randerson, J.T. The Global Fire Atlas of Individual Fire Size, Duration, Speed and Direction. *Earth Syst. Sci. Data* **2019**, *11*, 529–552. [[CrossRef](#)]
20. Balch, J.K.; St. Denis, L.A.; Mahood, A.L.; Mietkiewicz, N.P.; Williams, T.M.; McGlinchy, J.; Cook, M.C. FIRED (Fire Events Delineation): An Open, Flexible Algorithm and Database of US Fire Events Derived from the MODIS Burned Area Product (2001–2019). *Remote Sens.* **2020**, *12*, 3498. [[CrossRef](#)]
21. Artés, T.; Oom, D.; de Rigo, D.; Durrant, T.H.; Maianti, P.; Libertà, G.; San-Miguel-Ayán, J. A Global Wildfire Dataset for the Analysis of Fire Regimes and Fire Behaviour. *Sci. Data* **2019**, *6*, 296. [[CrossRef](#)]
22. Miller, J.D.; Thode, A.E. Quantifying Burn Severity in a Heterogeneous Landscape with a Relative Version of the Delta Normalized Burn Ratio (DNBR). *Remote Sens. Environ.* **2007**, *109*, 66–80. [[CrossRef](#)]
23. Key, C.H.; Benson, N.C. Landscape Assessment (LA). In *FIREMON: Fire Effects Monitoring and Inventory System*; Gen. Tech. Rep. RMRS-GTR-164-CD; U.S. Department of Agriculture, Forest Service, Rocky Mountain Research Station: Ft. Collins, CO, USA, 2006; p. LA-1-55.
24. Parks, S.; Dillon, G.; Miller, C. A New Metric for Quantifying Burn Severity: The Relativized Burn Ratio. *Remote Sens.* **2014**, *6*, 1827–1844. [[CrossRef](#)]
25. Thirgood, J.V. *Man and the Mediterranean Forest: A History of Resource Depletion*; Academic Press: London, UK; New York, NY, USA, 1981; ISBN 978-0-12-687250-7.
26. Peñuelas, J.; Sardans, J. Global Change and Forest Disturbances in the Mediterranean Basin: Breakthroughs, Knowledge Gaps, and Recommendations. *Forests* **2021**, *12*, 603. [[CrossRef](#)]
27. Keeley, J.E.; Bond, W.J.; Bradstock, R.A.; Pausas, J.G.; Rundel, P.W. *Fire in Mediterranean Ecosystems: Ecology, Evolution and Management*; Cambridge University Press: Cambridge, UK, 2011; ISBN 978-1-139-03309-1.

28. Camarero, J.J.; Sánchez-Salguero, R.; Sangüesa-Barreda, G.; Lechuga, V.; Viñepla, B.; Seco, J.I.; Taïqui, L.; Carreira, J.A.; Linares, J.C. Drought, Axe and Goats. More Variable and Synchronized Growth Forecasts Worsening Dieback in Moroccan Atlas Cedar Forests. *Sci. Total Environ.* **2021**, *765*, 142752. [[CrossRef](#)] [[PubMed](#)]
29. Aoulad-Sidi-Mhend, A.; Maaté, A.; Amri, I.; Hlila, R.; Chakiri, S.; Maaté, S.; Martín-Martín, M. The Geological Heritage of the Talassemtane National Park and the Ghomara Coast Natural Area (NW of Morocco). *Geoheritage* **2019**, *11*, 1005–1025. [[CrossRef](#)]
30. Ben-Said, M.; Ghallab, A.; Lamrhari, H.; Carreira, J.A.; Linares, J.C.; Taïqui, L. Characterizing Spatial Structure of Abies Marocana Forest through Point Pattern Analysis. *For. Syst.* **2020**, *29*, e014. [[CrossRef](#)]
31. Chouvy, P.-A.; Macfarlane, J. Agricultural Innovations in Morocco's Cannabis Industry. *Int. J. Drug Policy* **2018**, *58*, 85–91. [[CrossRef](#)]
32. Haut Commissariat aux Eaux et Forêts et à la Lutte Contre la Désertification (HCEFLCD). *Elaboration Du Plan d'Aménagement et de Gestion Du Parc National de Talassemtane, Version Provisoire—Juin 2018*; Ressources Naturelles BETAF: Rabat, Morocco, 2018; Volume I, 157p, Volume II, 120p.
33. European Center for Medium-Range Weather Forecasts. Available online: <https://en.climate-data.org/africa/morocco/chefchaouen/chefchaouen-3997/> (accessed on 6 April 2022).
34. Benabid, A. *Flore et Écosystèmes du Maroc: Évaluation et Préservation de la Biodiversité*; Éd. Ibis Presses: Paris, France, 2000; ISBN 978-2-910728-13-7.
35. Taïqui, L.; Martín Cantarino, C. Eléments Historiques d'analyse Écologique Des Paysages Montagneux Du Rif Occidental (Maroc). *MDTRRA* **1997**, *1997*, 23–35. [[CrossRef](#)]
36. Giglio, L.; Boschetti, L.; Roy, D.P.; Humber, M.L.; Justice, C.O. The Collection 6 MODIS Burned Area Mapping Algorithm and Product. *Remote Sens. Environ.* **2018**, *217*, 72–85. [[CrossRef](#)]
37. Vadrevu, K.P.; Lasko, K.; Giglio, L.; Schroeder, W.; Biswas, S.; Justice, C. Trends in Vegetation Fires in South and Southeast Asian Countries. *Sci. Rep.* **2019**, *9*, 7422. [[CrossRef](#)]
38. Schroeder, W.; Oliva, P.; Giglio, L.; Csizsar, I.A. The New VIIRS 375 m Active Fire Detection Data Product: Algorithm Description and Initial Assessment. *Remote Sens. Environ.* **2014**, *143*, 85–96. [[CrossRef](#)]
39. Boschetti, L.; Roy, D.P.; Giglio, L.; Huang, H.; Zubkova, M.; Humber, M.L. Global Validation of the Collection 6 MODIS Burned Area Product. *Remote Sens. Environ.* **2019**, *235*, 111490. [[CrossRef](#)] [[PubMed](#)]
40. Song, C.; Woodcock, C.E.; Seto, K.C.; Lenney, M.P.; Macomber, S.A. Classification and Change Detection Using Landsat TM Data. *Remote Sens. Environ.* **2001**, *75*, 230–244. [[CrossRef](#)]
41. Cocke, A.E.; Fulé, P.Z.; Crouse, J.E. Comparison of Burn Severity Assessments Using Differenced Normalized Burn Ratio and Ground Data. *Int. J. Wildland Fire* **2005**, *14*, 189. [[CrossRef](#)]
42. Singleton, M.P.; Thode, A.E.; Sánchez Meador, A.J.; Iniguez, J.M. Increasing Trends in High-Severity Fire in the Southwestern USA from 1984 to 2015. *For. Ecol. Manag.* **2019**, *433*, 709–719. [[CrossRef](#)]
43. Zahrae Redouan, F.; Benitez, G.; Aboubakr, B.; Bakkouri Bassma, E.; Maria Picone, R.; Crisafulli, A.; Ben Driss, A.; Kadiri, M.; Molero Messa, J.; Merzouki, A. The Status and Perception of Medicinal Plants by Local Population of Talassemtane National Park (Northern Morocco). *Casp. J. Environ. Sci.* **2020**, *18*, 131–147.
44. Rhattas, M.; Zidane, L.; Douira, A. Écotourisme Dans Le Parc Naturel De Talassemtane (Nord Du Maroc). *J. Anim. Plant Sci.* **2015**, *24*, 3752–3767.
45. Taïqui, L. Evolution Récente de La Structure Du Paysage Du Bassin de Chefchaouen (1958–1986). In *Mutations des Milieux Ruraux dans les Montagnes Rifaines (Maroc)*; Rif, G.R.G., Ed.; Série Etudes Spatiales n°2; Faculté des Lettres & Sciences Humaines de Tétouan: Martil, Morocco, 2005.
46. Dadashi, S. What Is a Fire? Identifying Individual Fire Events Using the MODIS Burned Area Product. Master's Thesis, University of Colorado Boulder, Boulder, CO, USA, 2018.
47. Fusco, E.J.; Finn, J.T.; Abatzoglou, J.T.; Balch, J.K.; Dadashi, S.; Bradley, B.A. Detection Rates and Biases of Fire Observations from MODIS and Agency Reports in the Conterminous United States. *Remote Sens. Environ.* **2019**, *220*, 30–40. [[CrossRef](#)]
48. Zidane, I.; Lhissou, R.; Bouli, A.; Mabrouki, M. An Improved Algorithm for Mapping Burnt Areas in the Mediterranean Forest Landscape of Morocco. *J. For. Res.* **2019**, *30*, 981–992. [[CrossRef](#)]
49. Laurent, P.; Mouillot, F.; Yue, C.; Ciaï, P.; Moreno, M.V.; Nogueira, J.M.P. FRY, a Global Database of Fire Patch Functional Traits Derived from Space-Borne Burned Area Products. *Sci. Data* **2018**, *5*, 180132. [[CrossRef](#)]
50. Humber, M.L.; Boschetti, L.; Giglio, L.; Justice, C.O. Spatial and Temporal Intercomparison of Four Global Burned Area Products. *Int. J. Digit. Earth* **2019**, *12*, 460–484. [[CrossRef](#)] [[PubMed](#)]
51. van Wees, D.; van der Werf, G.R.; Randerson, J.T.; Andela, N.; Chen, Y.; Morton, D.C. The Role of Fire in Global Forest Loss Dynamics. *Glob. Chang. Biol.* **2021**, *27*, 2377–2391. [[CrossRef](#)] [[PubMed](#)]
52. Aplet, G.H.; Laven, R.D.; Smith, F.W. Patterns of Community Dynamics in Colorado Engelmann Spruce-Subalpine Fir Forests. *Ecology* **1988**, *69*, 312–319. [[CrossRef](#)]
53. Esteban, L.G.; de Palacios, P.; Aguado, L.R.-L. *Abies Pinsapo* Forests in Spain and Morocco: Threats and Conservation. *Oryx* **2010**, *44*, 276–284. [[CrossRef](#)]
54. Mascarenhas, F.D.S.; Brown, I.F.; da Silva, S.S. Desmatamento e Incêndios Florestais Transformando a Realidade Da Reserva Extrativista Chico Mendes. *Desenvolvo. Meio Ambiente* **2018**, *48*, 236–262. [[CrossRef](#)]
55. Fernández-García, V.; Marcos, E.; Fulé, P.Z.; Reyes, O.; Santana, V.M.; Calvo, L. Fire Regimes Shape Diversity and Traits of Vegetation under Different Climatic Conditions. *Sci. Total Environ.* **2020**, *716*, 137137. [[CrossRef](#)]